number in the selected area to estimate percent area containing intravascular and extravasated EB as an approximate index of BBB breakdown. Image analysis was focused on the paramedian portion of the corpus callosum facing the dorsal part of the lateral ventricle, because WM lesions were most intense in this region.[3]

Statistical Analysis

All data are presented as means±SE. A one-factor ANOVA followed by Fisher protected least significant difference procedure was used to compare the differences between groups. P values <0.05 were considered to be statistically significant.

Results

The amount of total MMP-2 in the forebrain extracts was comparable between the vehicle-treated and AG3340-injected rats after BCAO as assessed using the Biotrak Activity Assay System. The percentage of activated MMP-2 was only 7% on day 3 after the sham operation but was elevated to approximately 80% on day 3 after the BCAO (supplemental Figure I, available online at http://stroke.ahajournals.org). We also confirmed almost complete suppression of MMP-2 activation with AG3340 administration.

The operation was successful in rats (n=40) except 3, which developed convulsions and was killed within 7 days, and in mice (n=62) except 4, which developed cerebral infarction. These animals with unsuccessful operations were excluded from the statistical analysis. In the vehicle-treated animals, severe WM lesions, as shown by an increased number of disarranged nerve fibers and vacuolation, were found on day 14 after the BCAO in the optic nerve, medial part of the corpus callosum (Figure 1B and 1E), the internal capsule, and the fiber bundles of the caudoputamen. In such WM regions, the number of Ricinus communis agglutinin-1-positive microglia and GFAP-positive astroglia increased (2- to 3-fold) on day 3 after the BCAO (Figure 1H and 1K). Both WM lesions and gliosis were less severe in the AG3340-treated animals (Figure 1C, 1F, 1I, 1L, 1P through 1R, and Table 1).

The BBB integrity in rats subjected to BCAO was also assessed by the immunostaining for IgM. IgM-immunoreactive glial cells represent those cells that have taken up the serum proteins, which leaked into the brain parenchyma, and their number serves as an indicator of BBB dysfunction.[8] Some IgM-immunoreactive glial cells were found in the vicinity of the microvessels in the corpus callosum in the vehicle-treated animals on day 3 after the BCAO (Figure 1R), suggesting BBB dysfunction in this region. In contrast, much fewer IgM-immunoreactive glia were found in the same area of the AG3340-treated animals (Figure 1O and 1R).

These results strengthen the notion that MMPs play a role in BBB impairment and WM lesions. To further elucidate the roles of MMPs in the WM damage after chronic cerebral hypoperfusion, we applied BCAS (the established technique for mice hypoperfusion)[3] for mice lacking functional MMP-2 gene (MMP-2-null mice), which showed no obvious developmental abnormalities[10] or brain anomalies[11] and examined its effects using histochemical methods. The reduction of CBF after BCAS was comparable between wild-type and MMP-2-null mice. The CBF reductions (wild-type versus MMP-2-null; mean±SE %, n=3 each) were 42.5±4.3% versus 39.1±3.2% (2 hours after BCAS), 38.1±4.3 versus 39.4±4.0 (3 days), 35.2±4.6 versus 33.6±6.2 (7 days), 20.8±1.4 versus 26.9±3.1 (14 days), and 11.2±3.0 versus 24.0±4.0 (30 days). In wild-type mice, MMP-2-immunoreactive glial cells increased after BCAS compared with sham-operated mice (Figure 2A and 2B). MMP-9-immunoreactive cells were not induced after BCAS in both wild-type (Figure 2C and 2D) and MMP-2-null mice (Figure 2E). Consistently, zymography using forebrain homogenates revealed only a faint band of MMP-9 in the samples after BCAS for 3 days in both wild-type and MMP-2-null mice (n=4), whereas a robust band was found in the sample from a mouse with an incidental cerebral infarction after BCAS (Figure 2G). A band of MMP-2 was detected in the samples in wild-type mice but not in MMP-2-null mice after BCAS (n=4). However, zymography using such homogenates failed to show the upregulation of MMP-2 after 3 days of BCAS; regional upregulation of MMP-2 in the WM seemed obscured.

Klüver-Barrera staining revealed that WM lesions were predominant in the corpus callosum, caudoputamen, and internal capsule but not in optic tract on day 30 after BCAS in the wild-type mice. The medial part of the corpus callosum adjacent to the lateral ventricles was most severely affected (Figure 3E). In MMP-2-null mice, such WM lesions were far less severe (Figure 3I; Table 2). The mouse model showed little damage to the visual pathway and no difference was found between the wild-type mice and MMP-2-null mice after the operation. This may be attributable to the fact that BCAS in mice induces a milder decrease in the CBF than in the rat model and maintains a residual blood flow within the common carotid arteries and its branch, the ophthalmic artery.

In the wild-type mice on day 14 after BCAS, numerous activated microglia, as visualized by immunostaining with anti-MHC class II antibodies, were found in some WM regions (Figure 3F). In addition, the number of GFAP-immunoreactive astroglia increased in these mice (Figure 3G). In the MMP-2-null mice, the number of microglia and astroglia was much fewer in the WM as compared with the wild-type animals (Figure 3J, 3K, 3P, 3Q). Thus, both WM lesions and glial activation after chronic hypoperfusion were dramatically reduced in the MMP-2-null mice. There was no difference of the number of microglia, astroglia, and IgM-positive cells in optic tract (Figure 3P).

The BBB integrity in mice subjected to BCAS was assessed by the immunostaining for IgM and EB extravasation assay. After BCAS, the number of IgM-positive cells increased in the WM of the wild-type mice (Figure 3H) as compared with the sham-operated wild-type animals (Figure 3D). Intriguingly, the IgM-immunoreactive cells significantly decreased in the WM of MMP-2-null mice after BCAS (Figure 3L and 3R). IgM-immunoreactive cells were identified as astroglia based on their colabeling with GFAP in the perivascular areas (Figure 3L through 3O). Three days after BCAS, EB apparently leaked into the perivascular area in the corpus callosum (Figure 4B) and the cerebral cortex (data not shown). This extravasation was most notable in the paramedian portion of the corpus callosum. At all time points after BCAS, no extravasation of EB could be detected in the MMP-2-null mice (Figure 4C). The estimated percent area

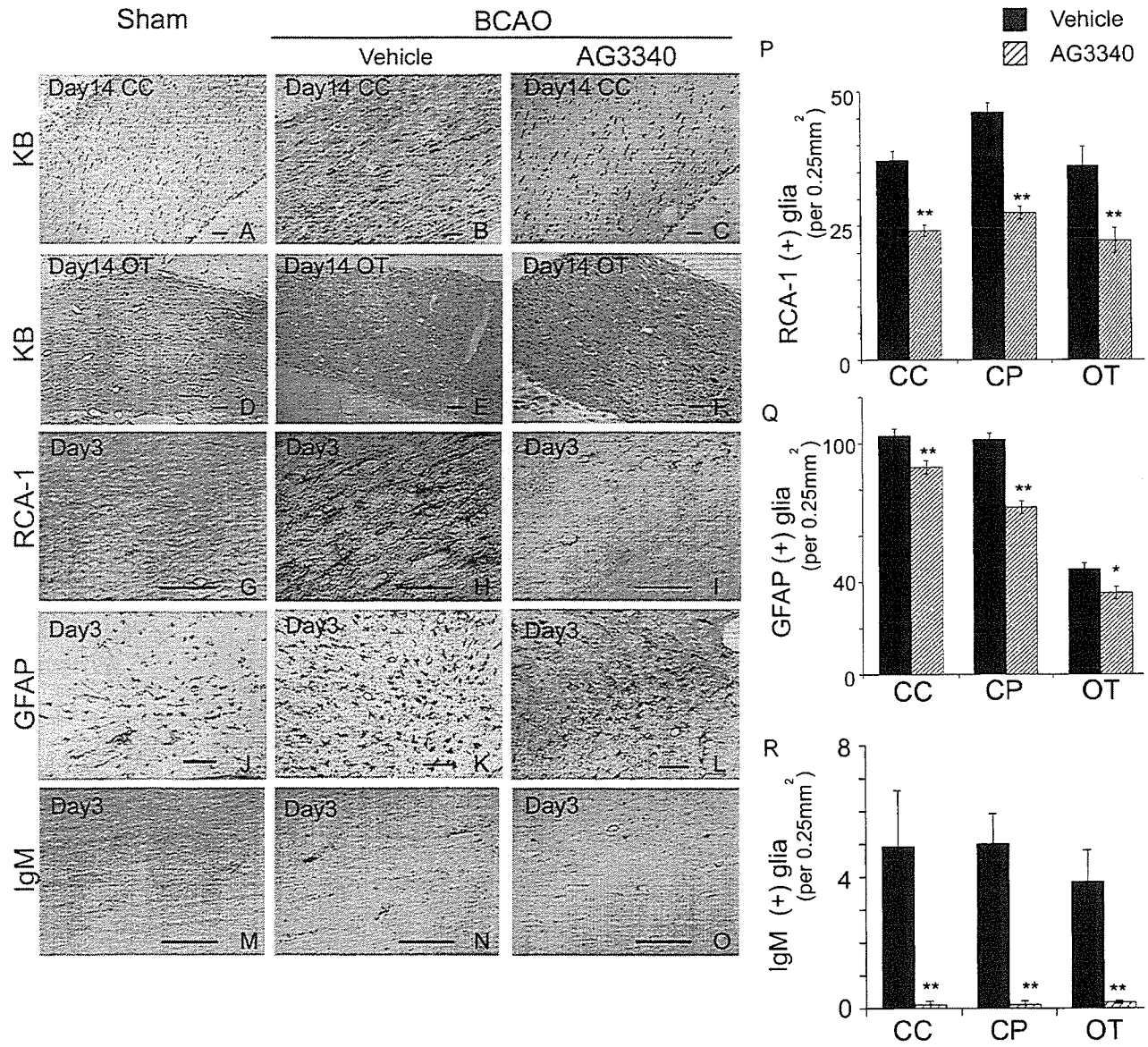

Figure 1. Histologic evaluation of the WM lesions in rats after chronic cerebral hypoperfusion with or without AG3340-treatment. A through O, Klüver-Barrera staining on day 14 (A through F; myelin sheath) or immunostaining on day 3 for Ricinus communis agglutinin-1 (G through I; microglia), GFAP (J through L; astroglia), or IgM (M through O) of the corpus callosum (A through C, G through O) and optic tract (D through F) of rats that had undergone sham operation (A, D, G, J, M) or BCAO operation, which had been treated either with vehicle (B, E, H, K, N) or AG3340 (C, F, I, L, O). Scale bar, 50 μm. (P through R) A histogram representing the density of cells immunoreactive for Ricinus communis agglutinin-1 (P), GFAP (Q), or IgM (R) in sections from the corpus callosum (CC), caudoputamen (CP), and optic tract (OT) in rats 3 days after a BCAO (n=4 each; *$P<0.05$, **$P<0.01$).

stained with EB was approximately 8% in wild-type mice after BCAS, which significantly reduced to 2% in MMP-2-null mice after BCAS (Figure 4D). Taken together, these results indicated that loss of MMP-2 alleviated BBB damage after BCAS and suggested a causative role for MMP-2 in the WM lesions after hypoperfusion.

TABLE 1. Histologic Grading of the WM Lesions in Untreated and AG3340-Treated Rats on Day 14 After BCAO

	Corpus Callosum	Caudoputamen	Optic Tract
Vehicle, N=5	1.3±045	1.4±0.54	2.6±0.55
AG3340, N=4	0.5±0.4*	0.63±0.25*	1.13±0.63*

*$P<0.05$.

Discussion

The synthetic MMP inhibitor AG3340 is known to inhibit several MMP family members, including MMP-2 (Ki=0.05 nmol/L), MMP-9 (0.26 nmol/L), MMP-13 (0.03 nmol/L), and MT1-MMP (0.33 nmol/L).[12] As a lipophilic, low-molecular-weight (Mr 423.5) compound, AG3340 can readily cross the BBB.[12] Using this compound, we have demonstrated that AG3340 shows protective effects against the WM lesions after chronic cerebral hypoperfusion in rats. This is consistent with our previous data using the same model, which showed a correlation of WM lesions with MMP-2 upregulation.[8] Then, AG3340 may have reduced the severity of WM lesions by inhibiting MMP-2 activation. In support of this notion,

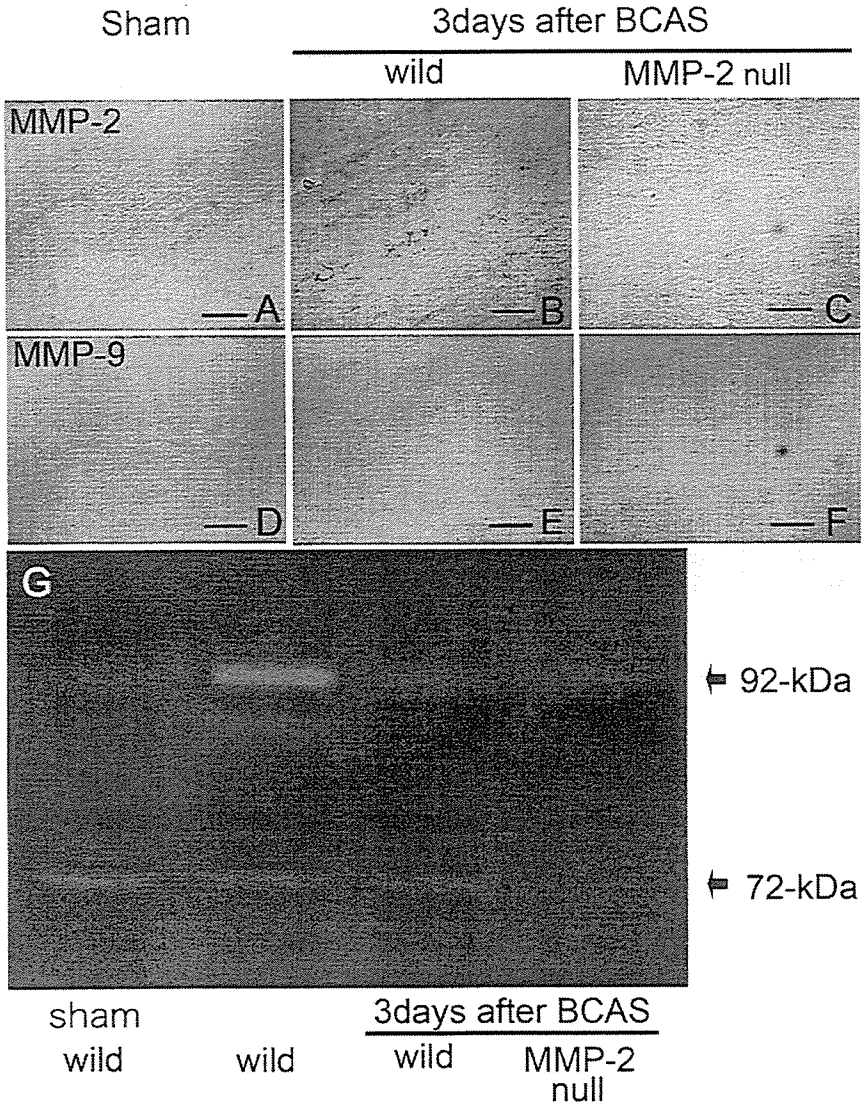

Figure 2. A through F, Immunohistochemical analysis for MMP-2 (A through C) and MMP-9 (D through F) in the corpus callosum of wild-type mice (A, B, D, E) or MMP-2-null mice (C, F) on day 3 after sham operation or BCAS (B, D). G, Zymography assay of the samples from a mouse with incidental cerebral infarction (CI), a wild-type mouse and an MMP-2-null mouse 3 days after BCAS. Note the absence of compensatory upregulation of MMP-9 in MMP-2-null mice.

genetic deletion of MMP-2 attenuated the WM lesions after chronic cerebral hypoperfusion in mice. These data jointly suggest that MMP-2 upregulation plays a major role in the WM lesions.

Previous studies have established the importance of the upregulation and activation of MMPs in acute brain ischemia.[13–15] Among the members of the MMP family (n≥20), MMP-9 is of particular interest in the context of acute brain ischemia, because the selective upregulation of MMP-9 has been observed in the brains of patients with stroke.[15] More importantly, the neuronal damage after cerebral ischemia was attenuated in the MMP-9-null mice compared with the wild-type mice.[16] Furthermore, Heo et al demonstrated association of MMP-9 upregulation with hemorrhagic transformation in the nonhuman primates.[17] Thus, MMP-9 upregulation may contribute to the BBB damage and infarct size, especially in the acute setting. Although previous study demonstrated the upregulation of MMP-9 in MMP-2-null mice,[18] no upregulation of MMP-9 was observed in our model, which suggested a negligible role of MMP-9 in chronic cerebral hypoperfusion.

What then would be the role of MMPs in cerebral ischemia? Hamann et al reported disappearance of the basal lamina around the microvessels during cerebral ischemia and reperfusion.[7] Fukuda et al demonstrated that the ischemic primate brain contained elevated levels of activity enough to digest basal lamina components such as type IV collagen.[19] In fact, Heo et al indicated that MMP-2 upregulated significantly by 1 hour after MCAO[18] and was persistently elevated thereafter in primates, and Chan et al demonstrated the upregulation of activation system for latent MMP-2 after focal cerebral ischemia.[20] These findings support the hypothesis that excessive degradation of the vascular basal lamina is a mechanism by which MMP triggers BBB dysfunction, edema, hemorrhage. The most marked extravasation of Evans blue in the paramedian portion of the corpus callosum facing the lateral ventricle was consistent with a previous report on a rat model of chronic cerebral hypoperfusion[21] and further indicated a vulnerability of the BBB in this area. In the case of chronic hypoperfusion, a previous study suggested the association of MMP-2 but not MMP-9 upregulation with BBB disruption. Consistently, Rosenberg et al showed that the activated

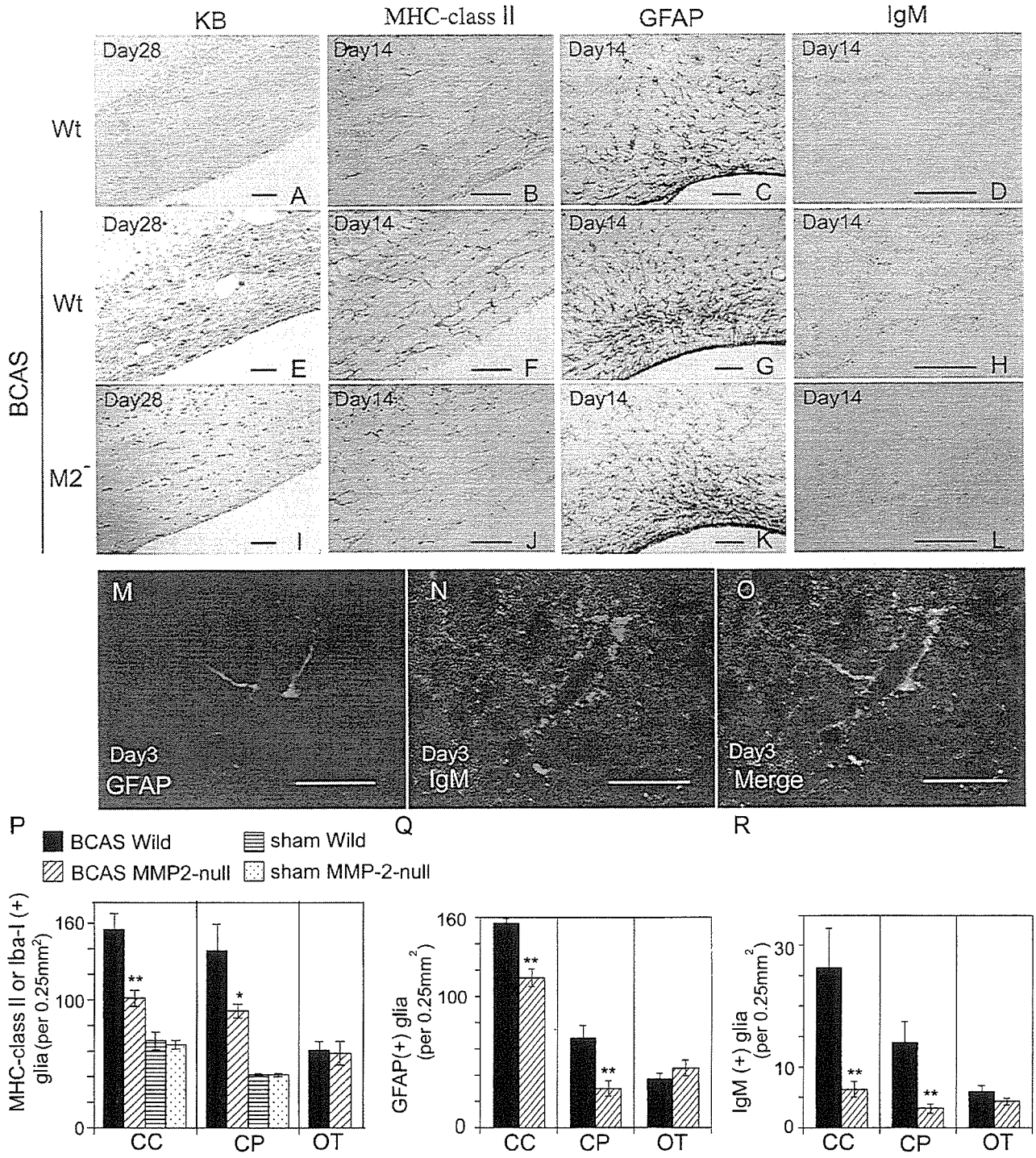

Figure 3. Histologic evaluation of the WM lesions in wild-type and MMP-2-null mice after BCAS. A through L, Klüver-Barrera staining 28 days after BCAS (A, E, I) and immunostaining 14 days after BCAS for MHC class II (B, F, J), GFAP (C, G, K), or IgM (D, H, L) of corpus callosum sections from wild-type (Wt) mice (A through H) or MMP-2-null ($M2^-$) mice (I through L) that had undergone either a sham operation (A through D) or BCAS (E through L). Note that MMP-2 gene knockout recover the decrease of Klüver-Barrera staining in the WM after BCAS (compare E with I) and glial activation (compare F with J for microglia and G with K for astroglia). Scale bar, 50 μm. M through O, Double staining with GFAP and IgM of the WM lesions in wild-type mice after BCAS. IgM was observed on endfeet of GFAP-positive glia (O). Scale bar, 10 μm. P through R, A histogram representing the density of cells immunoreactive for MHC-class II or Iba-I (P), GFAP (Q), or IgM (R) in sections from the corpus callosum (CC), caudoputamen (CP), and optic tract (OT) of mice that had undergone BCAS (n=6 each; $^*P<0.05$, $^{**}P<0.01$). For the microglial count, anti-MHC-class II antibodies were used for mice with BCAS operation, whereas anti-Iba-I antibodies were used for mice with sham operation (P). Note that glial activation was not observed in the optic tract, being consistent with the absence of rarefaction of this structure.

TABLE 2. Histologic Grading of the WM Lesions in Wild-Type and MMP-2-Null Mice on Day 30 After BCAS

	Corpus Callosum	Caudoputamen	Anterior Commissure
Wild-type, N=6	1.5±0.8	1.3±0.58	0.5±0.5
MMP-2-null, N=6	0.5±0.8*	0.58±0.37*	0±0

*$P<0.05$.

astroglia and microglia/macrophages around the arterioles expressed MMP-2 and MMP-3, but not MMP-9, in the brains of patients with vascular dementia.[6]

Caplan[22] proposed that the major pathologic features of WM lesions such as demyelination and gliosis may result from a BBB dysfunction, which allows the leakage of proteins and fluid through the compromised barrier of the penetrating arteries. This hypothetical pathway is consistent with our present findings. Given the overlapping substrate specificity between MMP-2 and MMP-9, in the case of chronic cerebral hypoperfusion, MMP-2 may contribute to the BBB disruption through the excessive digestion of the vascular basal lamina and activation of glia. In addition, MMP-2 may be directly involved in demyelination associated with WM lesions, because MMP-2 can digest myelin more efficiently than MMP-9.[24]

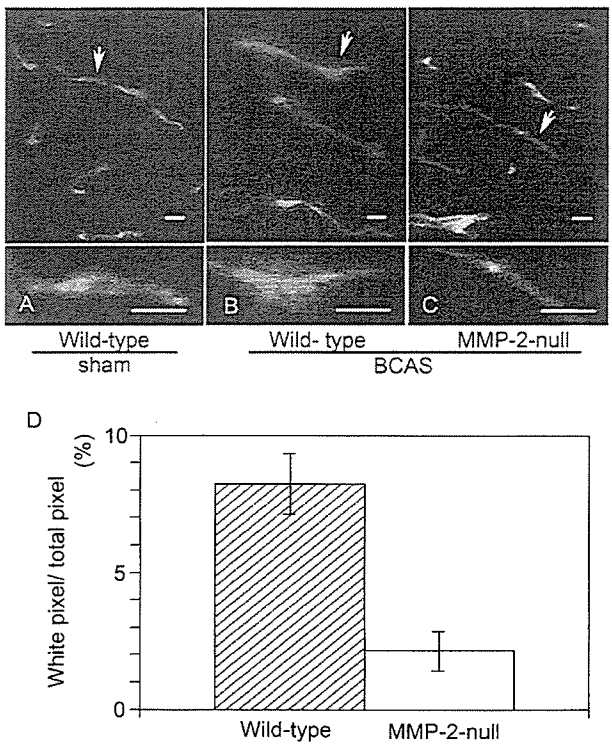

Figure 4. Evaluation of BBB dysfunction in the corpus callosum of mice. The Evans blue extravasation assay was performed on day 3 after a sham operation in wild-type mice (A) or on day 3 after BCAS in wild-type (B) and MMP-2-null mice (C). A magnified view of the area indicated by an arrow in the upper panel is shown in the lower panel (A through C). The experiments were repeated in triplicate with similar findings (n=4 each). Scale bar, 100 μm. A histogram representing the degree of Evans blue extravasation as an approximate index of BBB breakdown (see "Methods") (D).

In conclusion, the present study has provided direct evidence that MMP-2 is involved in the pathogenesis of WM lesions in the mouse model. Although the species difference between rodents and humans should be taken into consideration, our data also suggest the potential value of MMP inhibitors in preventing subcortical ischemic vascular dementia resulting from BBB dysfunction and chronic cerebral ischemia in humans. Activation of MMP-2 is reported to participate in matrix injury during focal cerebral ischemia. An elucidation of the exact roles of MMP-2 in BBB disruption may also provide information useful in developing strategies for controlling neuroinflammation in general.

Acknowledgments

The authors are indebted to Miss Nakabayashi for her excellent technical assistance.

Disclosures

None.

References

1. Meguro K, Hatazawa J, Yamaguchi T, Itoh M, Matsuzawa T, Ono S, Miyazawa H, Hishinuma T, Yanai K, Sekita Y. Cerebral circulation and oxygen metabolism associated with subcortical perivascular hyperintensity as shown by magnetic resonance imaging. *Ann Neurol.* 1990;28:378–383.
2. Wakita H, Tomimoto H, Akiguchi I, Kimura J. Glial activation and white matter changes in the rat brain induced by chronic cerebral hypoperfusion: an immunohistochemical study. *Acta Neuropathol.* 1994;87:484–492.
3. Shibata M, Ohtani R, Ihara M, Tomimoto H. White matter lesions and glial activation in a novel mouse model of chronic cerebral hypoperfusion. *Stroke.* 2004;35:2598–2603.
4. Sternlicht MD, Werb Z. How matric metalloproteinases regulate cell behavior. *Annu Rev Cell Dev Biol.* 2001;17:463–516.
5. Clark AW, Krekoski CA, Bou SS, Chapman KR, Edwards DR. Increased gelatinase A (MMP-2) and gelatinase B (MMP-9) activities in human brain after focal ischemia. *Neurosci Lett.* 1997;238:53–56.
6. Rosenberg GA, Sullivan N, Esiri MM. White matter damage is associated with matrix metalloproteinases in vascular dementia. *Stroke.* 2001;32:1162–1168.
7. Hamann GF, Okada Y, Fitridge R, del Zoppo GJ. Microvascular basal lamina antigens disappear during cerebral ischemia and reperfusion. *Stroke.* 1995;26:2120–2126.
8. Ihara M, Tomimoto H, Kinoshita M, Oh J, Noda M, Wakita H, Akiguchi I, Shibasaki H. Chronic cerebral hypoperfusion induces MMP-2 but not MMP-9 expression in the microglia and vascular endothelium of the white matter. *J Cereb Blood Flow Metab.* 2001;21:828–834.
9. Price A, Shi Q, Morris D, Wilcox ME, Brasher PM, Rewcastle NB, Shalinsky D, Zou H, Appelt K, Johnston RN, Yong VW, Edwards D, Forsyth P. Marked inhibition of tumor growth in a malignant glioma tumor model by a novel synthetic matrix metalloproteinase inhibitor AG3340. *Clin Cancer Res.* 1999;4:845–854.
10. Itoh T, Ikeda T, Gomi H, Nakao S, Suzuki T, Itohara S. Unaltered secretion of beta-amyloid precursor protein in gelatinase A (matrix metalloproteinase 2)-deficient mice. *J Biol Chem.* 1997;272:22389–22392.
11. Asahi M, Sumii T, Fini ME, Itohara S, Lo EH. Matrix metalloproteinase 2 gene knockout has no effect on acute brain injury after focal ischemia. *Neuroreport.* 2001;12:3003–3007.
12. Shalinsky DR, Brekken J, Zou H, McDermott CD, Forsyth P, Edwards D, Margosiak S, Bender S, Truitt G, Wood A, Varki NM, Appelt K. Broad antitumor and antiangiogenic activities of AG3340, a potent and selective MMP inhibitor undergoing advanced oncology clinical trials. *Ann N Y Acad Sci.* 1999;878:236–270.
13. Rosenberg GA, Navratil M, Barone F, Feuerstein G. Proteolytic cascade enzymes increase in focal cerebral ischemia in rat. *J Cereb Blood Flow Metab.* 1996;16:360–366.

14. Horstmann S, Kalb P, Koziol J, Gardner H, Wagner S. Profiles of matrix metalloproteinases, their inhibitors, and laminin in stroke patients: influence of different therapies. *Stroke*. 2003;34:2165–2170.
15. Maier CM, Hsieh L, Yu F, Bracci P, Chan PH. Matrix metalloproteinase-9 and myeloperoxidase expression: quantitative analysis by antigen immunohistochemistry in a model of transient focal cerebral ischemia. *Stroke*. 2004; 5:1169–1174.
16. Lee SR, Tsuji K, Lee SR, Lo EH. Role of matrix metalloproteinase in delayed neuronal damage after transient global ischemia. *J Neurosci*. 2004;24:671–678.
17. Heo JH, Lucero J, Abumiya T, Koziol JA, Copeland BR, del Zoppo GJ. Matrix metalloproteinases increase very early during experimental focal cerebral ischemia. *J Cereb Blood Flow Metab*. 1999;19:624–633.
18. Esparza J, Kruse M, Lee J, Michaud M, Madri JA. MMP-2 null mice exhibit an early onset and severe experimental autoimmune encephalomyelitis due to an increase in MMP-9 expression and activity. *FASEB J*. 2004;18:1682–1691.
19. Fukuda S, Fini CA, Mabuchi T, Koziol JA, Eggleston LL Jr, del Zoppo GJ. Focal cerebral ischemia induces active proteases that degrade microvascular matrix. *Stroke*. 2004;35:998–1004.
20. Chang DI, Hosomi N, Lucero J, Heo JH, Abumiya T, Mazar AP. Activation system for latent matrix metalloproteinase-2 are upregulated immediately after focal cerebral ischemia. *J Cereb Blood Flow Metab*. 2003;23:1408–1419.
21. Ueno M, Tomimoto H, Akiguchi I, Wakita H, Sakamoto H. Blood–brain barrier disruption in white matter lesions in a rat model of chronic cerebral hypoperfusion. *J Cereb Blood Flow Metab*. 2002; 22:97–104.
22. Caplan LR. Dilatative arteriopathy (dolichoectasia): what is known and not known. *Ann Neurol*. 2005;57:472–479.
23. Chandler S, Coates R, Gearing A, Lury J, Wells G, Bone E. Matrix metalloproteinases degrade myelin basic protein. *Neurosci Lett*. 1995; 201:223–226.

血管性認知症とイメージング

Molecular imaging of vascular dementia

京都大学医学部附属病院神経内科医長
Hidekazu Tomimoto 冨本秀和

Summary

血管性認知症(vascular dementia；VaD)は，大血管の障害に起因する多発梗塞性認知症(multi infarct dementia；MID)と小血管性認知症に分類される。小血管性認知症は臨床病理学的観点から，多発ラクナ梗塞，ビンスワンガー病，strategic infarct dementia の3病型に分類されるが，前2者は白質病変とラクナ梗塞を基本病変とし subcortical vascular dementia(SVD)と総称される。SVD は緩徐進行性の経過をとることが多くアルツハイマー病との鑑別が問題になるが，MRI を含む神経機能画像の特徴から多くは鑑別が可能である。Strategic infarct dementia は記憶に重要な皮質下部位のラクナ梗塞と関連し，SVD の発症は前頭葉を中心とする皮質機能の低下と相関するが，いずれも皮質・皮質下のネットワーク障害で説明可能である。本稿では，VaD の多くを占める小血管性認知症のイメージングについて概説した。

Key words

- 血管性認知症
- 白質病変
- ビンスワンガー病
- subcortical vascular dementia(SVD)
- magnetic resonance imaging(MRI)

1 はじめに

血管性認知症(vascular dementia；VaD)は大血管の循環障害に起因する多発梗塞性認知症(multi infarct dementia；MID)と小血管性認知症に分類される。MID はアテローム血栓性梗塞や心原性脳塞栓症などが原因となり，大血管の閉塞の結果，主として大脳皮質領域に脳梗塞が多発する。したがって，運動機能障害も高度であることが多く，神経イメージングは梗塞部位の所見を反映することになる。

一方，小血管性認知症では白質病変やラクナ梗塞の多発にしたがって認知症が進行する。小血管性認知症は病変分布や臨床病理学的観点から，①多発ラクナ梗塞，②ビンスワンガー病，③ strategic infarct dementia の3病型に分類される。ビンスワンガー病は広範な白質病変を特徴とするが，多発ラクナ梗塞でも多かれ少なかれ白質病変を伴うことが多く，両者の境界は不明確といわざるをえない。このような理由から，両者を併せて subcortical vascular dementia(SVD)とする立場があり，このタイプの VaD は本邦では VaD 全体の過半数を占めている[1]。

SVD の約半数は明らかな卒中発作を伴わず，緩徐に神経症候が増悪する[2]。したがって，緩徐進行性に増悪する認知症を診た場合，SVD とアルツハイマー病(Alzheimer's disease；AD)の鑑別はしばしば困難であり，両

疾患の鑑別をいかに行うかは重要な問題である。一方，ADではラクナ梗塞や白質病変などの血管病変が高率に合併する。病因論的にも両疾患に共通の危険因子が多く指摘されており，ADの血管説も提唱されている。以上の観点から，本稿ではSVDとADの鑑別を画像診断の立場からいかに行うかについて述べ，さらにVaDの分子イメージングの現状について概説を試みた。

II SVDとアルツハイマー病の画像による鑑別

1．Magnetic resonance imaging(MRI)の立場から

SVDとADの確実な鑑別は，現時点では病理診断による他はない。われわれの剖検症例の成績では，剖検242症例中，脳血管障害(cerebrovascular disease；CVD)65例，AD 33例であり，両者の合併は13例にみられた。しかし，CVDのうちfibrohyalinosis，angionecrosisなどの小血管病変を高度に有するビンスワンガー病に限ってみると7例であり，このうち老人斑，神経原線維変化などの老人性変化が併存し，ADの病理診断基準に該当した症例は皆無であった。したがって，両疾患が病因論的に関連する可能性はあるが，本態的には別個の病態と考えられる。

ADの画像診断はアミロイドイメージングを中心に急速な展開をみせており，近未来的に解決が期待されるが，詳細については他稿を参照されたい。一方，SVDのMRIは白質病変とラクナ梗塞の多発によって特徴づけられる。白質病変はMRI T_2強調画像(またはFLAIR画像)で高輝度の病変であるが，必ずしも病理変化に対応しないとの指摘がある[3]。しかし，MRI所見と死後剖検脳を対比した多くの報告では，白質病変は髄鞘・軸索の脱落，グリア細胞のびまん性の変化，血管周囲腔の拡大，不完全梗塞に対応するとされている。

白質病変は加齢に伴って増加し，高血圧，CVDなどの危険因子があると高率となる。ADでは白質病変の頻度が増加するとの報告が多いが，健常対照と比較して有意差がないとする報告もある。HanyuらはMR拡散強調画像で，同年齢の対照と比べAD患者では側頭葉白質の拡散異方性が低下すると報告している[4]。Gootjesらの検討では健常高齢者，AD，VaDの3群について白質病変の容積比を算出し，ADは健常高齢者の2倍，VaDで16倍と高率であった。一方，白質病変の分布は前頭葉，頭頂葉に目立ち，この傾向は健常高齢者，AD，VaDに共通であった[5]。以上より，白質病変の分布パターンから両疾患を鑑別することは困難であるが，白質病変が非常に高度な例はVaDの可能性が高いと推測される。

2．SVDとアルツハイマー病の鑑別 —神経機能画像の立場から

白質病変はVaDの責任病変と指摘されているが，同程度の白質病変があっても認知機能低下の程度は一定しない。その理由として，白質病変は直接的に認知機能障害を惹起するわけではなく，ネットワーク障害を介して皮質の神経細胞機能を障害するためと推定されている。実際，認知機能の低下は白質病変やラクナ梗塞と相関せず，皮質機能を反映する皮質血流や糖代謝の低下と相関するとの報告がある[6]。

無症候性の白質病変では，脳血流は白質病変と逆相関して低下する傾向にある。また，認知症を伴う白質病変では，脳血流は前頭葉を中心に有意に低下する[7]。ポジトロンCT(positron emission tomography；PET)の検討においては，無症候性の白質病変では脳血流の低下に比較して脳酸素代謝率($CMRO_2$)は維持されている。これは細胞レベルで酸素摂取率(OEF)が上昇し代償していることを意味する。一方，認知症を呈する白質病変ではOEFの代償性亢進は消失し，$CMRO_2$が低下する[8]。

VaDの脳循環代謝をADと比較すると，VaDでは帯状回，上前頭回を含む前頭葉に低下がみられ，ADでは後部帯状回を含む頭頂葉・側頭葉に顕著である。また，CO_2負荷に対する血管反応性はVaDでは著明に低下するが，ADでは正常であるという[9]。われわれの脳SPECT(single-photon emission tomography)を用いた検討でも，起立負荷に対する血管反応性は虚血性白質病変が高度な症例では早期から障害されていた(図1)。

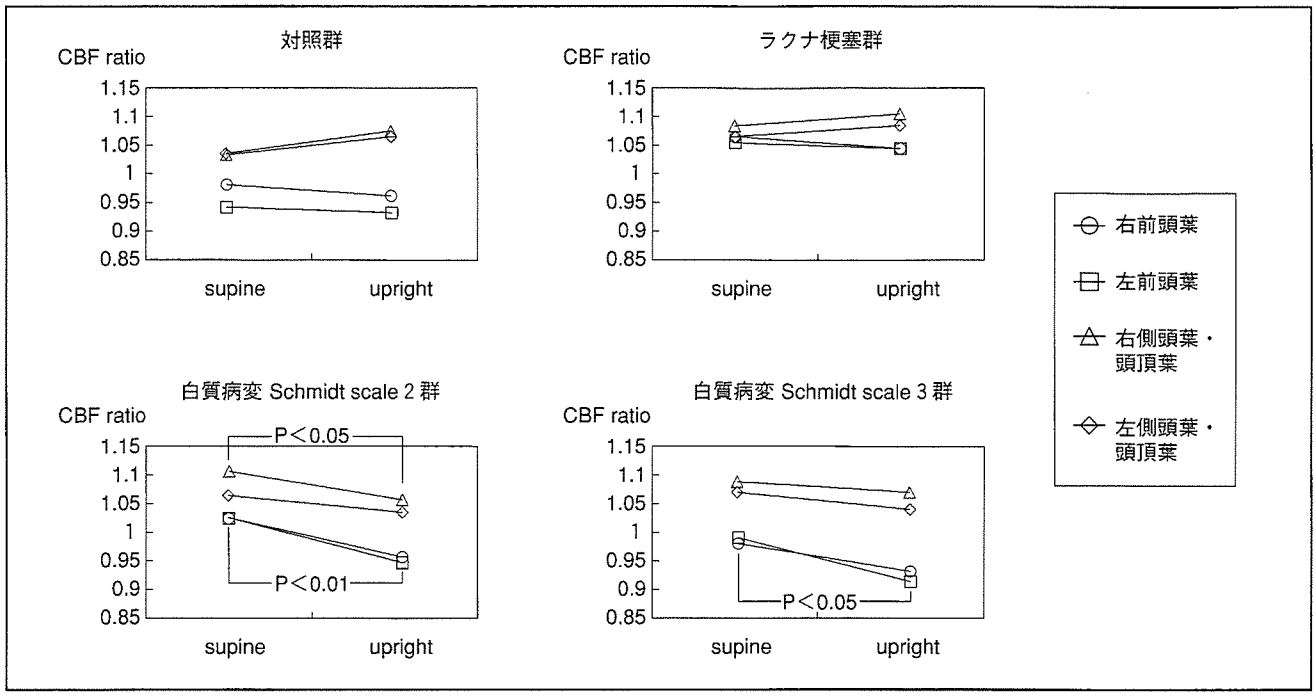

図1　脳血流SPECTで検討した起立負荷前後の脳血管反応性の変化
脳血流の指標(CBF ratio)は起立負荷後，白質病変 Schmidt scale 2 群では前頭葉，側頭葉・頭頂葉で低下した。また，白質病変 Schmidt scale 3 群では前頭葉で低下した。これに対し白質病変を有さない対照群，ラクナ梗塞群では変化を認めなかった。
(文献10)より引用)

Ⅲ 分子イメージングの血管性認知症への応用

最近の欧州の多施設共同研究 LADIS(Leukoaraiosis and Disability in the Elderly study)の結果では，白質病変容積と認知機能には相関関係を認めたものの，Fazekas スケールなどの一般的な白質病変スケールを用いた場合には有意でなかった。その原因として，白質病変容積が高度になると白質病変スケールは認知機能との相関が悪くなるという天井効果が指摘されている[11]。天井効果の理由として，同じ白質病変容積であっても病変局所の重症度，すなわち脱髄や軸索障害の程度が異なるため，認知機能に及ぼす影響が異なる可能性が考えられる。

MR スペクトロスコピー(magnetic resonance spectroscopy；MRS)を用いた白質病変の評価では，神経細胞に特異的に含まれる N-acetylaspartate(NAA)，エネルギー代謝の中間産物である creatine/phosphocreatine(Cr)，および主に細胞膜の崩壊産生に関わる物質である choline-containing compounds(Cho)のピークを検出できる。NAA/Cr 比は軸索障害，Cho/Cr 比は髄鞘障害の指標と考えられるが，SVD では認知機能正常の白質病変群と比べて NAA/Cr 比が低下，Cho/Cr 比は上昇し軸索障害・脱髄の存在が示唆される(**図2A, B**)[12]。NAA/Cr 比の低下は SVD 患者では前頭葉，頭頂葉が中心で，ラクナ梗塞，白質病変が存在すると増悪する。また，視床にラクナ梗塞が存在すると線維連絡が密な前頭葉で顕著に低下するが，頭頂葉では変化せず，皮質・皮質下ネットワークの障害を支持する結果である[13]。

白質病変スケールの天井効果の問題を克服するため，われわれは MR 拡散テンソル画像を用い，白質病変の

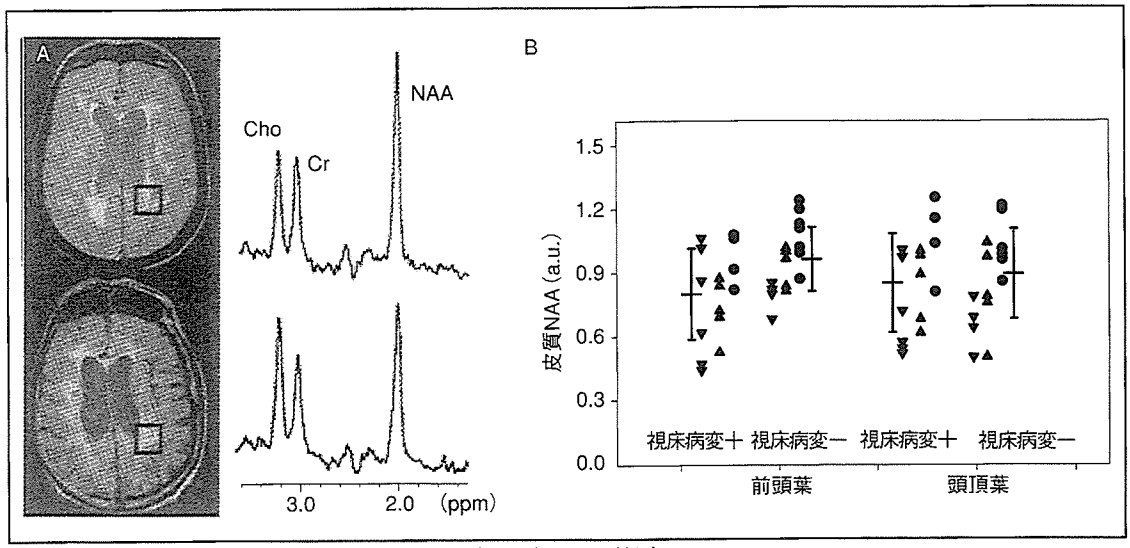

図2　SVD患者脳のMRスペクトロスコピー(MRS)による検討
A：無症候性白質病変を有する患者(上)とビンスワンガー病患者(下)の白質部のMRS。ビンスワンガー病ではNAA/Cr比が低下しCho/Cr比が上昇しており，白質病変の質的相違が示唆される(文献12)より引用)。
B：視床病変の有無による皮質NAA/Cr比の変化。低下は前頭葉において有意である。▼はSVD群，▲はアルツハイマー病群，●は認知機能正常のラクナ梗塞群を示す(文献13)より引用)。

異方性比率(fractional anisotropy；FA)を測定している。FA値は水分子の拡散に一定の方向性が認められる程度を数値化したものであり，三次元方向への拡散が等しい場合は0，一方向に限られる場合は1となる。その分布をFA mapとして表示することで，脳組織内の水分子の拡散異方性の低下を非侵襲的に可視化し，脱髄などに伴う組織構築の変化を評価することができる。同様の方法を用いたO'Sullivanらの報告によると，FA値は白質病変スケールと比較して実行機能と良好な相関を示している[14]。

Ⅳ　ラクナ梗塞・白質病変と神経ネットワーク障害

白質線維は皮質間を結ぶ連合線維，対応する大脳半球領域間を結ぶ交連線維，皮質・皮質下構造を連絡する投射線維により構成される。これらの線維はラクナ梗塞あるいは白質病変によって傷害されうるが，記憶に重要な特定の皮質下部位の障害によって認知機能の低下が起こる場合と，びまん性の神経ネットワーク障害の結果として皮質機能の低下をきたす場合がある[15]。

記憶に重要な解剖学的構造がラクナ梗塞によって傷害され，急性発症の健忘症を生じる場合は，strategic infarct dementiaと呼ばれる。これらには，①polar thalamic artery(視床極動脈)，②paramedian thalamic artery(傍正中視床動脈)，③後大脳動脈近位部から分枝する海馬動脈などの支配血管が関与する。脳血流はその投射部位と関連して低下し，特有のパターンを呈する。

視床極動脈の障害では，視床前核を中心に視床内髄板，乳頭体視床路が傷害される。視床前核，乳頭体視床路は記憶に重要なPapez circuitの構成要素であり，脳血流は前頭葉，側頭葉で広範に低下する。傍正中視床動脈の障害では，背内側核，正中中心核，傍束核などの核群と視床内髄板，前視床束を経由して内側前頭皮質へ投射する経路，下視床束を経由し島皮質，前頭・側頭葉，扁桃核へ投射する経路が傷害される。背内側核から扁桃核への経路は認知機能に密接に関連するbasolateral limbic circuit(Yakovlev)の一部を構成し，脳血流は内側前頭

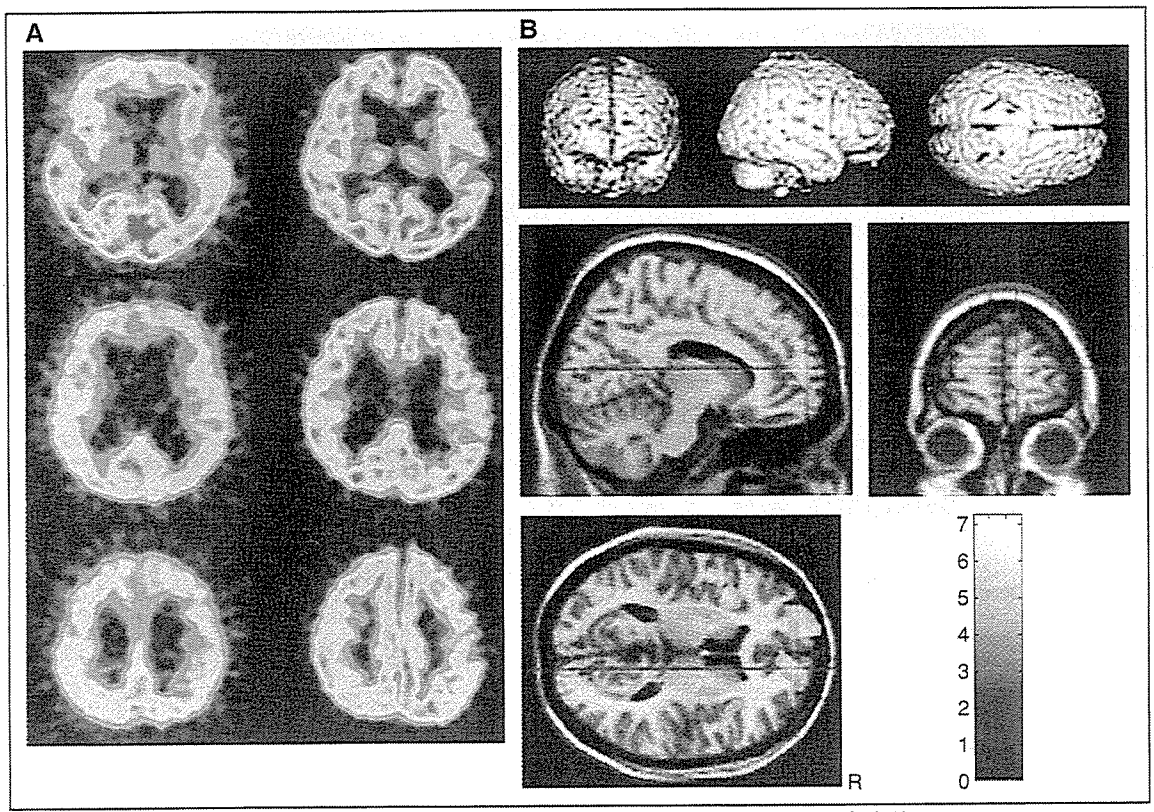

図3　ビンスワンガー病患者と無症候性白質病変を有する患者における FMZ の分布容積
A：ビンスワンガー病患者(左：70歳男性)と無症候性大脳白質病変を有する患者(右：79歳男性)における^{11}C-FMZ PET 像。ビンスワンガー病患者では FMZ の取り込みが前頭葉，側頭葉，頭頂葉で低下している。
B：Statistical parametric mapping(SPM)によるビンスワンガー病と無症候性大脳白質病変を有する患者間の FMZ 分布容積の比較。ビンスワンガー病患者では，前頭葉の中でも前頭極領域と島前方領域に FMZ の分布容積の低下が認められる。
(文献18)より引用)

葉，前部帯状回，扁桃核を含む側頭葉で低下する[16]。Tatemichi らは，内包膝部の小梗塞で背内側核から前視床束，下視床束への出力線維を傷害し，前頭葉を中心に傍正中視床動脈の場合と類似の血流障害が起こるとしている[17]。当然のことではあるが，SVD の患者でもこれらの血管領域に傷害が加われば認知症の階段状の増悪が認められる。

一方，びまん性白質病変が皮質機能の低下を惹起する可能性があり，この点についてわれわれは直接的証明を行っている[18]。フルマゼニル(FMZ)はベンゾジアゼピン受容体のリガンドである。脳酸素代謝は脳血流の低下によって二次的に変化する可能性を否定できないのに対し，FMZ の分布容積は神経細胞の $GABA_A$受容体密度を反映することから，'neuronal integrity' を直接反映するマーカーとされる。無症候の白質病変脳と比較し認知症を有する白質病変脳の FMZ 分布容積は，前頭葉，側頭葉，頭頂葉で低下しており，大脳皮質における広範な neuronal integrity の障害が示唆される(図3A，B)。Statistical parametric mapping(SPM)で評価すると前頭極領域と島前方領域に有意な FMZ 分布容積の低下があり，両領域が注意機構に関与している領域であることから，白質病変が皮質領域の機能低下を介して認知症の発症に関与していることが示唆される。

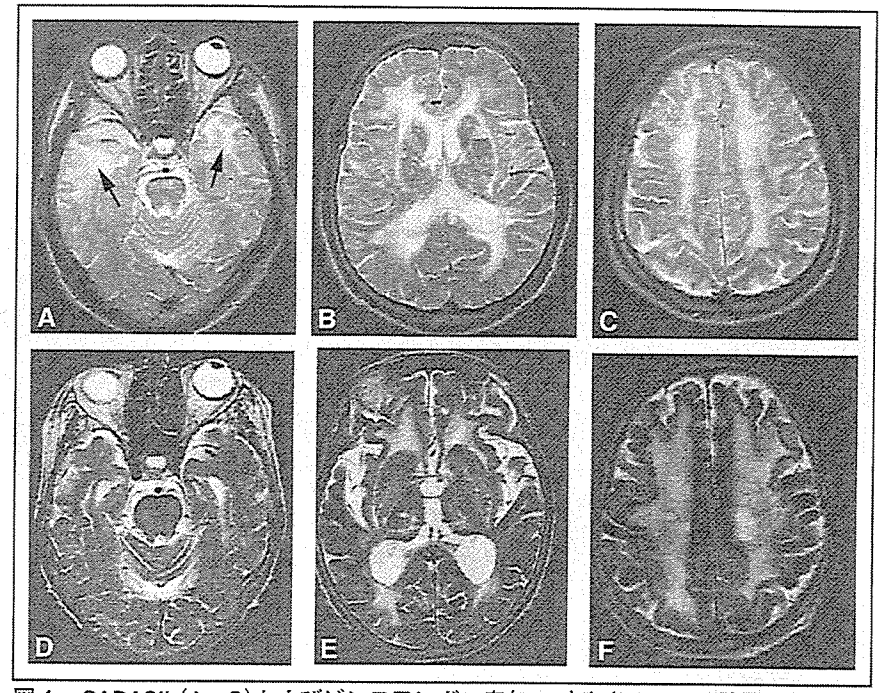

図4　CADASIL(A～C)およびビンスワンガー病(D～F)患者のMR T_2 強調画像
矢印(A)は前側頭極の白質病変を示す。

(文献22)より引用)

V 血管性認知症とコリン神経ネットワーク

VaDでは，コリン神経の脱落がADほど高度ではないが，認められる。前脳基底部のマイネルト基底核から上行するコリン神経は，外包を経由して大脳皮質に投射する。外包は白質病変の好発部位であるため，SVDではコリン神経路の障害が認められる[19]。白質病変スケールと認知機能障害の間に直線的な相関関係はみられないが，Boctiらはコリン神経路を特異的に評価するCHIPS(Cholinergic Pathways HyperIntensities Scale)を用いることで良好な相関が得られたと報告している[20]。大脳皮質に投射するコリン神経の脱落は認知機能低下を引き起こすが，その機序として神経細胞への直接作用はもちろんのこと，アセチルコリンの脳血管拡張作用の低下を介して皮質血流を低下させる可能性も指摘されている。

最後に，遺伝性にVaDをきたすcerebral autosomal dominant arteriopathy with subcortical infarcts and leukoencephalopathy(CADASIL)でもコリン神経の脱落がある[21]。白質病変の分布には非遺伝性のSVDと比較して明確な相違があり，CADASILでは早期から前側頭極に白質病変が出現するのが特徴とされている[22](図4)。

VI むすび

本稿ではVaDのイメージング全般について紹介し，加えて分子イメージングに関する最新の知見を紹介した。今後，分子イメージングの進歩がVaDの診断精度の向上と病態解析に寄与することが期待される。

文　献

1) Yanagihara T：Vascular dementia in Japan. Ann N Y Acad Sci **977**：24-28, 2002
2) Yoshitake T, Kiyohara Y, Kato I, et al：Incidence and

risk factors of vascular dementia and Alzheimer's disease in a defined elderly Japanese population ; The Hisayama Study. Neurology **45** : 1161-1168, 1995
3) Grafton ST, Sumi SM, Stimac GK, et al : Comparison of postmortem magnetic resonance imaging and neuropathologic findings in the cerebral white matter. Arch Neurol **48** : 293-298, 1991
4) Hanyu H, Sakurai H, Iwamoto T, et al : Diffusion-weighted MR imaging of the hippocampus and temporal white matter in Alzheimer's disease. J Neurol Sci **156** : 195-200, 1998
5) Gootjes L, Teipel SJ, Zebuhr Y, et al : Regional distribution of white matter hyperintensities in vascular dementia, Alzheimer's disease and healthy aging. Dement Geriatr Cogn Disord **18** : 180-188, 2004
6) Sabri O, Ringelstein EB, Hellwig D, et al : Neuropsychological impairment correlates with hypoperfusion and hypometabolism but not with severity of white matter lesions on MRI in patients with cerebral microangiopathy. Stroke **30** : 556-566, 1999
7) Meguro K, Hatazawa J, Yamaguchi T, et al : Cerebral circulation and oxygen metabolism associated with subclinical periventricular hyperintensity as shown by magnetic resonance imaging. Ann Neurol **28** : 378-383, 1990
8) Yao H, Sadoshima S, Ibayashi S, et al : Leukoaraiosis and dementia in hypertensive patients. Stroke **23** : 1673-1677, 1992
9) Nagata K, Maruya H, Yuya H, et al : Can PET data differentiate Alzheimer's disease from vascular dementia ? Ann N Y Acad Sci **903** : 252-261, 2000
10) Ohtani R, Tomimoto H, Kawasaki T, et al : Cerebral vasomotor reactivity to postural change is impaired in patients with cerebrovascular white matter lesions. J Neurol **250** : 412-417, 2003
11) van Straaten EC, Fazekas F, Rostrup E, et al : Impact of white matter hyperintensities scoring method on correlations with clinical data ; The LADIS Study. Stroke **37** : 836-840, 2006
12) Brooks WM, Wesley MH, Kodituwakku PW, et al : ^{1}H-MRS differentiates white matter hyperintensities in subcortical arteriosclerotic encephalopathy from those in normal elderly. Stroke **28** : 1940-1943, 1997
13) Schuff N, Capizzano AA, Du AT, et al : Different patterns of N-acetylaspartate loss in subcortical ischemic vascular dementia and AD. Neurology **61** : 358-364, 2003
14) O'Sullivan M, Morris RG, Huckstep B, et al : Diffusion tensor MRI correlates with executive dysfunction in patients with ischaemic leukoaraiosis. J Neurol Neurosurg Psychiatry **75** : 441-447, 2004
15) 冨本秀和 : 白質病変と認知機能障害 ; 血管性痴呆をめぐって. 認知神経科学 **7** : 230-239, 2005
16) Mori E, Ishii K, Hashimoto M, et al : Role of functional brain imaging in the evaluation of vascualr dementia. Alzheimer Dis Assoc Disord **13**(Suppl. 3) : S91-S101, 1999
17) Tatemichi TK, Desmond DW, Prohovnik I, et al : Confusion and memory loss from capsular genu infarction ; A thalamocortical disconnection syndrome ? Neurology **42** : 1966-1979, 1992
18) Ihara M, Tomimoto H, Ishizu K, et al : Decrease in cortical benzodiazepine receptors in symptomatic patients with leukoaraiosis ; A positron emission tomography study. Stroke **35** : 942-947, 2004
19) Tomimoto H, Ohtani R, Shibata M, et al : Loss of cholinergic pathways in vascular dementia of the Binswanger type. Dement Geriatr Cogn Disord **19** : 282-288, 2005
20) Bocti C, Swartz RH, Gao FQ, et al : A new visual rating scale to assess strategic white matter hyperintensities within cholinergic pathways in dementia. Stroke **36** : 2126-2131, 2005
21) Mesulam M, Siddique T, Cohen B : Cholinergic denervation in a pure multi-infarct state ; Observations on CADASIL. Neurology **60** : 1183-1185, 2003
22) Tomimoto H, Ohtani R, Wakita H, et al : Small artery dementia in Japan ; Radiological differences between CADASIL, leukoaraiosis and Binswanger's disease. Dement Geriatr Cogn Disord **21** : 162-169, 2006

available at www.sciencedirect.com
ScienceDirect
www.elsevier.com/locate/brainres
ELSEVIER
BRAIN RESEARCH

Research Report

Expression of S100 protein and protective effect of arundic acid on the rat brain in chronic cerebral hypoperfusion

Ryo Ohtani, Hidekazu Tomimoto, Hideaki Wakita, Hiroshi Kitaguchi, Kayoko Nakaji, Ryosuke Takahashi*

Department of Neurology, Kyoto University Graduate School of Medicine, Shogoin, Sakyo-ku, Kyoto 606-8507, Japan

ARTICLE INFO

Article history:
Accepted 30 November 2006
Available online 8 January 2007

Keywords:
White matter
Chronic cerebral hypoperfusion
Apoptosis
Astroglia
S100 protein
Arundic acid

ABSTRACT

S100 protein is expressed primarily by astroglia in the brain, and accumulates in and around the ischemic lesions. Arundic acid, a novel astroglia-modulating agent, is neuroprotective in acute cerebral infarction, whereas the protective effects remain unknown during chronic cerebral hypoperfusion. Rats undergoing chronic cerebral hypoperfusion were subjected to a bilateral ligation of the common carotid arteries, and were allowed to survive for 3, 7 and 14 days. The animals received a daily intraperitoneal injection of 5.0, 10.0 or 20.0 mg/kg of arundic acid, or vehicle, for 14 days. Alternatively, other groups of rats received a delayed intraperitoneal injection of 20.0 mg/kg of arundic acid or vehicle, which started from 1, 3 or 7 days after ligation and continued to 14 days. The degree of white matter (WM) lesions and the numerical density of S100 protein-immunoreactive astroglia were estimated. In the WM of rats with vehicle injections, the number of S100 protein-immunoreactive astroglia increased significantly after chronic cerebral hypoperfusion as compared to the sham-operation. A dosage of 10.0 and 20.0 mg/kg of arundic acid suppressed the numerical increase in S100 protein-immunoreactive astroglia and the WM lesions. These pathological changes were suppressed with delayed treatment up to 7 days in terms of astroglial activation, and up to 3 days in terms of the WM lesions. The protective effects of arundic acid against WM lesions were demonstrated in a dose-dependent manner, and even after postischemic treatments. These results suggest the potential usefulness of arundic acid in the treatment of cerebrovascular WM lesions.

1. Introduction

Ischemic white matter (WM) lesions are frequently observed in human cerebrovascular diseases (CVD), and are believed to be responsible for cognitive impairments in the elderly. It is believed that the occlusion of the small vessels results in lacunar cerebral infarction, and non-occlusive arteriopathy causes chronic cerebral hypoperfusion and WM lesions (Pantoni and Garcia, 1997). Indeed, WM lesions can be induced by a ligation of the bilateral common carotid arteries (CCAs) in rats, which leads to a 50–70% decrease in normal cerebral blood flow (CBF) over an extended period of time (Tsuchiya

* *Corresponding author*. Fax: +81 75 751 3766.
E-mail address: tomimoto@kuhp.kyoto-u.ac.jp (H. Tomimoto).

Abbreviations: WM, white matter; CVD, cerebrovascular disease; CCAs, common carotid arteries; CBF, cerebral blood flow; iNOS, inducible nitric oxide synthase; PBS, phosphate-buffered saline; KB, Klüver–Barrera; BBB, blood–brain barrier; TNFα, tumor necrosis factor alpha; COX2, cyclooxygenase 2

0006-8993/$ – see front matter © 2006 Elsevier B.V. All rights reserved.
doi:10.1016/j.brainres.2006.11.084

et al., 1992; Wakita et al., 1994). The myelins become rarefied with a proliferation of the astroglia and an activation of microglia, plus oligodendroglial cell death with DNA fragmentation in the WM (Tomimoto et al., 2003).

S100 is a 20-kDa Ca-binding protein composed of α and β subunits, and is primarily expressed by astroglia in the brain. This protein may play a dual role in the regulation of cell function, being beneficial to cells at low doses but detrimental at high doses (Hu et al., 1996). In human CVD, a significant correlation has been reported between the plasma concentration of S100 protein and the volume of the cerebral infarct (Aurell et al., 1991). Although low concentrations of S100 protein protect cultured neurons from glutamate-induced excitotoxic damage, a high concentration of this protein upregulates the expression of inducible nitric oxide synthase (iNOS) in cultured astroglia with the subsequent production of NO and death of astroglia and neurons (Hu et al., 1996, 1997; Murphy, 2000).

Indeed, arundic acid, an agent that inhibits the astrocytic synthesis of S100 (Asano et al., 2005), has been shown to be neuroprotective in a rat model of acute cerebral infarction (Tateishi et al., 2002). Arundic acid may interfere with the intricate pathways of astrocytic activation upstream to the mRNA expression of various proteins, and is considered to be a modulator of the gene expression and functions of astroglia (Asano et al., 2005; Shinagawa et al., 1999).

In the present study, we examined the protective effects of arundic acid on WM lesions during chronic cerebral hypoperfusion, and also investigated its therapeutic window for delayed treatment. Our results support the potential use of arundic acid as a therapeutic intervention in human cerebrovascular WM lesions with cognitive impairment.

2. Results

2.1. *Mortality rates and laboratory data*

In the first series of experiments, 1 out of 7 arundic acid-treated rats died at a dosage of 5.0 mg/kg (14.3%), and none died at dosages of 10.0 and 20.0 mg/kg (0.0%). The laboratory data (erythrocyte count, leukocyte count, GOT, GPT, BUN and creatinine levels) and rectal temperature were not significantly different between the vehicle-treated and arundic acid-treated rats (Table 1).

2.2. *Dose-dependent effect of arundic acid on S100 protein expression*

In the WM of the sham-operated animals, only a few astroglia showed positive immunostaining for the S100 protein. From 3 to 14 days after the operation, the brains of the vehicle-treated animals showed a numerical increase in astroglia, which were immunoreactive for S100 protein in various WM regions such as the optic nerve, optic tract, corpus callosum, and internal capsule (Figs. 1A–D). These S100 protein-immunoreactive astroglia increased in number after BCAO as compared to the sham-operated control group in these WM regions (Fig. 1E, Table 2).

In the 10.0 and 20.0 mg/kg arundic acid-treated rats, S100 protein-immunoreactive astroglia appeared to be less numerous in the WM regions as compared to the vehicle-treated animals for 14 days. In the semi-quantitative analysis, the number of S100 protein-immunoreactive astroglia was reduced in both 10.0 and 20.0 mg/kg arundic acid-treated groups as compared to the vehicle-treated group ($p<0.001$; Figs. 2A–D). The number of astroglia decreased in the 5.0, 10.0 and 20.0 mg/kg arundic acid-treated groups compared to the vehicle-treated group. The number was also reduced in the 20.0 mg/kg arundic acid-treated animals as compared to the 10.0 mg/kg arundic acid-treated animals ($p<0.05$), indicating a dose-dependent effect for arundic acid (Fig. 2E, Table 2).

2.3. *Dose-dependent effect of arundic acid on WM lesions*

This dose-related protective effect was similarly observed with respect to the WM lesions. In the 10.0 and 20.0 mg/kg arundic acid-treated groups, the scores were lower as compared to the vehicle-treated group (two-factor factorial ANOVA; $p<0.001$). There were no significant differences in grading scores between the 5.0 mg/kg arundic acid-treated group and vehicle-treated group. However, the 20.0 mg/kg arundic acid-treated animals showed a significant reduction ($p<0.05$) as compared to the 10.0 mg/kg arundic acid-treated animals (Fig. 2F, Table 2).

2.4. *Effects of delayed treatment*

In the delayed-treatment group, which started from 1, 3, or 7 days after the operation, the number of S100 protein-immunoreactive astroglia showed a significant decrease in the WM regions as compared to the vehicle-treated animals

Table 1 – Summary of the laboratory data in rats receiving vehicle or arundic acid

	Erythrocyte ($\times10^4$/mm^3) ($n=6$)	Leukocyte ($\times10^2$/mm^3) ($n=6$)	Thrombocyte ($\times10^3$/mm^3) ($n=6$)	GOT (IU/l) ($n=5$)	GPT (IU/l) ($n=6$)	BUN (mg/dl) ($n=5$)	Creatinine (mg/dl) ($n=6$)	Rectal temperature (°C) ($n=6$)
Vehicle	753.0±42.8	48.4±8.6	88.6±9.6	156.8±18.8	53.6±6.6	20.4±2.8	0.48±0.08	36.5±0.5
Arundic acid (5.0 mg/kg)	790.0±36.8	52.5±22.8	90.4±10.8	178.6±20.4	49.6±8.8	21.8±2.2	0.54±0.12	36.6±1.0
Arundic acid (10.0 mg/kg)	778.0±20.4	50.8±16.8	92.4±9.6	148.8±22.4	45.2±6.8	18.6±1.9	0.46±0.09	36.5±1.0
Arundic acid (20.0 mg/kg)	774.4±31.8	54.8±18.6	91.4±14.4	166.6±38.4	51.2±9.2	19.8±2.4	0.52±0.14	36.6±0.5

Values represent means±SD. n, number of animals. No significant differences were detected in the laboratory data between the arundic acid-treated group and the vehicle-treated group.

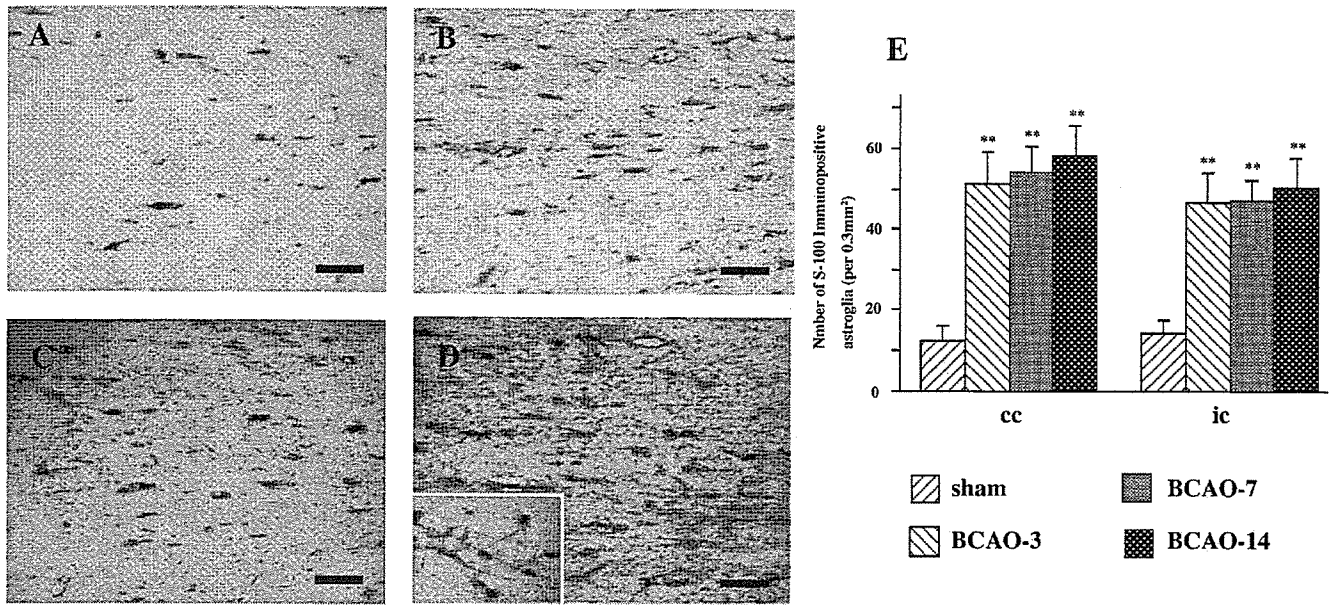

Fig. 1 – Photomicrographs of the immunohistochemical staining for S100 protein in the corpus callosum. The rats were subjected to a sham operation (A), or bilateral ligation of the carotid arteries for 3 days (B), 7 days (C) or 14 days (D). An inset in (D) indicates that S100 protein is intensely expressed in astroglial foot processes around the blood vessel. Bars indicate 100 μm. E: Histograms of the numerical densities of S100 protein-immunoreactive astroglia in the WM of the rats after a bilateral common carotid artery occlusion. Six animals were used in each group. The asterisks indicate statistical significance at $p<0.01$ by Mann–Whitney *U* test when compared with the sham-operated controls. cc, corpus callosum; ic, internal capsule.

for 14 days (Figs. 3A–E, Table 2). The WM lesions were less severe (two-factor factorial ANOVA; $p<0.001$) as compared to the vehicle-treated group in the groups starting at 1 day and 3 days after the operation (Fig. 3F, Table 2), but there were no significant changes in the group starting at 7 days.

3. Discussion

In the present study, we demonstrated a protective effect for arundic acid against astroglial activation and WM lesions during chronic cerebral hypoperfusion. Arundic acid suppressed both the activation of the astroglia and the WM lesions in a dose-dependent manner. Both the astroglial activation and WM lesions were suppressed at dosages over 10 mg/kg, whereas the dosage of 5.0 mg/kg suppressed the astroglial activation exclusively. Therefore, it is unlikely that the activation of the astroglia was secondary to the WM damage, but rather seems to be related to the causative mechanism.

Microglia and astroglia are activated in the WM aberrantly after chronic cerebral hypoperfusion (Wakita et al., 1994). This activation occurs in a manner that predicts the extent and severity of the subsequent WM damage, suggesting an important role of glial activation in the pathogenesis of WM lesions. In the susceptible WM, apoptosis of the oligodendroglia is induced with an upregulation of inflammatory cytokines including tumor necrosis factor alpha (TNFα), and free radicals released from activated microglia and astroglia (Tomimoto et al., 2003). In addition, the compromised BBB (Ueno et al., 2002) may allow the entry of macromolecules and other blood constituents such as proteases, immunoglobulins, complements, and cytokines into the perivascular WM tissues.

In studies using a neuronal and astroglia co-culture system, a high concentration of S100 protein upregulated NO release from the astroglia, which was shown to be neurotoxic

Table 2 – The number of S100 protein-immunoreactive astroglia in the white matter

		Corpus callosum				Internal capsule		
I. Temporal profile after BCAO	Sham	3 days	7 days	14 days	Sham	3 days	7 days	14 days
	12.3±3.5	51.3±7.8**	53.8±6.9**	58.1±7.3**	14.0±3.6	46.5±7.7**	47.0±5.2**	50.5±7.1**
II. Dose-dependent effect	Vehicle	5 mg/kg	10 mg/kg	20 mg/kg	Vehicle	5 mg/kg	10 mg/kg	20 mg/kg
	63.5±8.3	53.1±6.3**	35.3±6.2**	10.9±6.0**	54.9±8.4	33.0±7.1**	26.1±5**	21.9±5.7**
III. Effects of delayed treatment	Vehicle	Day 1	Day 3	Day 7	Vehicle	Day 1	Day 3	Day 7
	62.0±6.6	13.2±3.8**	18.2±5.1**	48.9±6.6**	54.5±7.1	21.9±3.1**	23.7±5.0**	42.2±6.3**

Values represent the number of S100 protein-immunoreactive astroglia in 0.3 mm^2 (means±SD).
** $p<0.01$ compared to the sham-operated (I) and the vehicle-treated (II and III) animals.

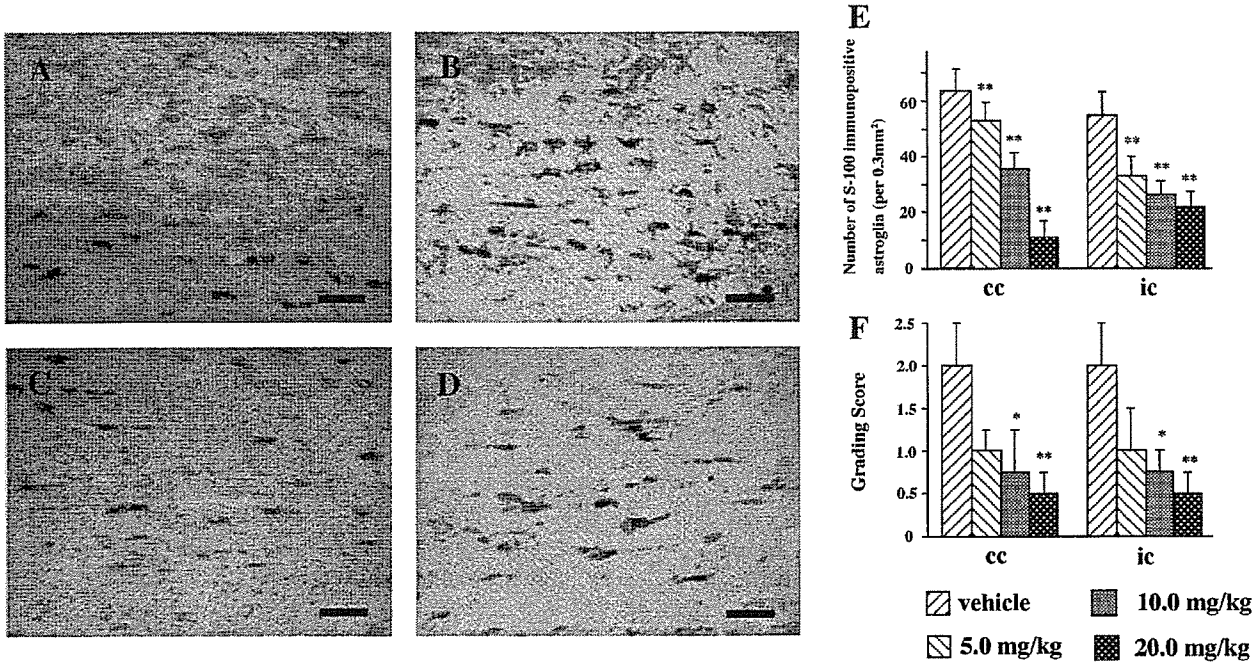

Fig. 2 – Photomicrographs of the immunohistochemical staining for S100 protein in the corpus callosum. The animals received an intraperitoneal injection of vehicle (A) or 5.0 mg/kg (B), 10.0 mg/kg (C) and 20.0 mg/kg (D) of arundic acid for 14 days. In the arundic acid-treated animals, astroglia immunoreactive for S100 protein were less numerous as compared with the vehicle-treated animals. Bars indicate 100 μm. The histograms show the numerical densities of S100 protein-immunoreactive astroglia (E), and the grading scores for the WM lesions (F) in rats receiving either vehicle or arundic acid for 14 days. $^{*}p<0.05$; $^{**}p<0.01$ by Fisher's protected least significant difference procedure, as compared to the vehicle-treated animals.

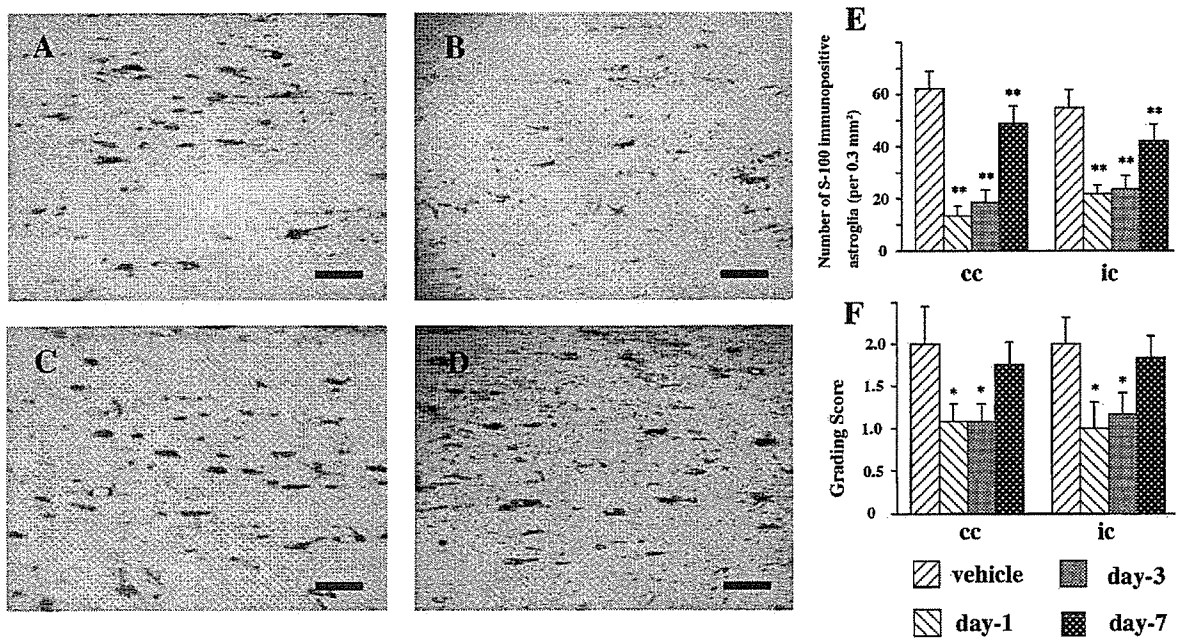

Fig. 3 – Photomicrographs of the immunohistochemical staining for S100 protein in the corpus callosum. The animals received an intraperitoneal injection of 20.0 mg/kg of arundic acid from 1 day (B), 3 days (C) or 7 days (D) after the operation, until 14 days. The control animals (A) received a daily injection of vehicle 1 day before the operation until 14 days. In the delayed treatment with arundic acid, the number of S100 protein-immunoreactive astroglia was significantly reduced as compared with the control animals. Bars indicate 100 μm. The histograms show the numerical density of S100 protein-immunoreactive astroglia (E) and the grading scores for the WM lesions (F) in rats receiving either vehicle or arundic acid from 1 day, 3 days or 7 days after the operation until 14 days. $^{*}p<0.05$; $^{**}p<0.01$ by Fisher's protected least significant difference procedure, as compared to the vehicle-treated animals.

(Hu et al., 1997; Nawashiro et al., 2000). Although the mechanism of responsible for this astroglial activation by a low concentration of S100 protein remains unclear, this protein is believed to be further activated by a positive feedback loop (Guo et al., 2001; Murphy, 2000). It is postulated that these excessively activated astroglia may cause secondary tissue damage by the production of cytotoxic cytokines such as TNFα, and cyclooxygenase 2 (COX2) and iNOS (Lam et al., 2001; Sharp et al., 2000). Indeed, the delayed expansion of the cerebral infarction was accompanied by astroglial activation as well as by an increased tissue level of S100 protein in the peri-infarct area. Thus, the astroglial overexpression of S100 protein is considered to play a pivotal role in infarct expansion by causing alterations in the activities of multiple intracellular signaling pathways and the expression of various downstream proteins (Asano et al., 2005; Matsui et al., 2002).

Several *in vitro* and *in vivo* studies have determined the pharmacological actions of arundic acid on astroglia. Arundic acid acts selectively on astroglia and modulates their activation, or prevents excessive activation that may be harmful to neighboring neurons. It does not act on neuronal cultures directly, but suppresses the changes induced in the co-cultured astroglia, such as an increase in S100β content, the secretion of nerve growth factor, a reduction in glutamate transporter (GLT-1 and GLAST) expression and the disappearance of GABAA receptors, in a dose-dependent manner, without affecting GFAP expression (Asano et al., 2005; Himeda et al., 2006; Katsumata et al., 1999; Matsui et al., 2002). In addition, arundic acid inhibits the expression of cyclooxygenase-2 or inducible nitric oxide synthase mRNA induced by lipopolysaccharide in cultured astroglia (Shimoda et al., 1998).

The dosage ranging from 5 to 20 mg/kg in the present study was comparable to that used in clinical application (8 mg/kg/h in acute stroke patients) (Pettigrew et al., in press). Furthermore, arundic acid was effective in delayed treatment starting from 7 days in terms of astroglial activation, and 3 days in terms of the WM lesions. This broad therapeutic time window is of clinical relevance, because the patients with subcortical vascular dementia, a form of vascular dementia characterized by diffuse WM lesions, frequently undergo a latent deterioration and hospitalization delay (Roman, 2005).

4. Experimental procedures

4.1. *Animals*

Chronic cerebral hypoperfusion was induced in male Wistar rats (150 to 200 g; Shimizu Laboratory Supplies Co. Ltd., Kyoto, Japan) as previously described (Wakita et al., 1994). The animals were anesthetized with sodium pentobarbital (25 mg/kg, i. p.) and were allowed spontaneous respiration throughout the surgical procedure. Through a midline cervical incision, both CCAs were exposed and double-ligated with silk sutures. Their rectal temperature was monitored and maintained between 36.0 and 37.0 °C during the surgical procedure, and the rats were kept in animal quarters with standard rodent chow and tap water *ad libitum* after the operation.

4.2. *Treatment with arundic acid*

The rats with vehicle (saline) treatment were sacrificed at 3, 7 and 14 days (body weight, 300 g; $n=6$, for each group) to study the temporal profile of the S100 protein-immunoractive astroglia and the WM lesions. In the first series of experiments with arundic acid, the animals received a daily intraperitoneal injection of 5.0, 10.0 or 20.0 mg/kg of arundic acid, or vehicle, from 1 day before the operation to 14 days afterwards ($n=6$ for each group). At 14 days after ligation, the animals were sacrificed and subjected to the experiments detailed below. The sham-operated animals were treated similarly to the operated ones, except the CCAs were not occluded. In the second series with a delayed-treatment, the animals received a daily intraperitoneal injection of 20.0 mg/kg of arundic acid or vehicle from 1 day, 3 days or 7 days after the operation until 14 days ($n=6$ for each group). At 14 days after ligation, the animals were sacrificed and subjected to the experiments detailed below. The control animals received a daily injection of vehicle 1 day after the operation until 14 days.

4.3. *Standard histological and immunohistochemical study*

After the operation, the animals were deeply anesthetized with sodium pentobarbital and were perfused transcardially with 0.01 mol/L phosphate-buffered saline (PBS), and then with a fixative containing 4% paraformaldehyde and 0.2% picric acid in 0.1 mol/L PB (pH 7.4). The brains were then stored in 20% sucrose in 0.1 mol/L PBS (pH 7.4). These specimens were embedded in paraffin and sliced into 2 μm-thick coronal sections. Klüver–Barrera (KB) staining was used to observe any histological changes. The severity of the WM lesions was graded as normal (grade 0), disarrangement of the nerve fibers (grade 1), formation of vacuoles (grade 2) and loss of myelinated fibers (grade 3) by two independent investigators blinded to the type of treatment, as described elsewhere (Wakita et al., 1994). For the immunohistochemistry, polyclonal antibodies directed against the S100 protein (diluted 1:1000; Dakopatts, 4.5 mg/L) were used in the present study. After incubation with the primary antibodies, the sections were treated with a biotinylated anti-rabbit antibody (IgG) (diluted 1:200; Vector Laboratories), and an avidin biotin complex (diluted 1:200; Vector Laboratories) in 20 mmol/L PBS containing 0.3% Triton-X. The sections were finally incubated in 0.01% diaminobenzidine tetrahydrochloride and 0.005% H_2O_2 in 50 mmol/L Tris HCl (pH 7.6). To test the specificity of the immunohistochemical reaction, coronal sections were treated with normal mouse IgG instead of the primary antibodies. The number of nuclei with S100 protein-immunoreactive cytoplasm was counted against a square test grid in 20 representative fields (per 0.3 mm^2) of the corpus callosum and internal capsule ($n=6$) by two independent investigators blinded to the type of treatments as described previously (Tomimoto et al., 1996).

4.4. *Statistical analysis*

The data were expressed as means±SD. Differences in rectal temperature between the groups were determined by a

repeated-measure ANOVA. Differences in terms of laboratory blood data were determined by a one-factor ANOVA between each group. Differences in the grading scores were determined by a two-factor factorial ANOVA followed by Fischer's protected least significant difference procedure between each group. The Kruskal–Wallis test followed by post-hoc test was used to compare the ischemic group with the sham-operated control group in the semiquantification for S100 protein-immunoreactive astroglia. A p value of <0.05 was considered to be statistically significant.

Acknowledgments

We appreciatively acknowledge Ono Pharmaceutical Co. Ltd., Osaka, Japan, for providing arundic acid (ONO-2506), and for helpful advice. This study was supported by a grant-in-aid for scientific research (C) (18590936) from the Japanese Ministry of Education, Culture, Sports, Science and Technology to H. T. and Dr. H. Saiki (Kitano Hospital, Osaka, Japan).

REFERENCES

Asano, T., Mori, T., Shimoda, T., Shinagawa, R., Satoh, S., Yada, N., Katsumata, S., Matsuda, S., Kagamiishi, Y., Tateishi, N., 2005. Arundic acid (ONO-2506) ameliorates delayed ischemic brain damage by preventing astrocytic overproduction of S100B. Curr. Drug Targets, CNS Neurol. Disord. 4, 127–142.

Aurell, A., Rosengren, E.L., Larlsson, B., Olsson, E.J., Zbornikova, V., Haglid, G.K., 1991. Determination of S-100 and glial fibrillary acidic protein concentrations in cerebrospinal fluid after brain infarction. Stroke 22, 1254–1258.

Guo, L., Sawkar, A., Zasadzki, M., Watterson, M.D., 2001. Similar activation of glial cultures from different rat brain regions by neuroinflammatory stimuli and downregulation of the activation by a new class of small molecule ligands. Neurobiol. Aging 22, 975–981.

Himeda, T., Kadoguchi, N., Kamiyama, Y., Kato, H., Maegawa, H., Araki, T., 2006. Neuroprotective effect of arundic acid, an astrocyte-modulating agent, in mouse brain against MPTP (1-methyl-4-phenyl-1,2,3,6-tetrahydropyridine) neurotoxicity. Neuropharmacology 50, 329–344.

Hu, J., Castets, F., Guevana, L.J., 1996. S100β stimulates inducible nitric oxide synthase activity and mRNA levels in rat cortical astrocytes. J. Biol. Chem. 271, 2543–2547.

Hu, J., Ferreia, A., 1997. S100β induces neuronal cell death through nitric oxide release from astrocytes. J. Neurochem. 69, 2294–2301.

Katsumata, S., Tateishi, N., Kagamiishi, Y., Shintaku, K., Hayakawa, T., Shimoda, T., Shinagawa, R., Akiyama, T., Katsube, N., 1999. Inhibitory effect of ONO-2506 on GABAA receptor disappearance in cultures astrocytes and ischemic brain. Abstr.-Soc. Neurosci. 25, 2108.

Lam, G.A., Koppal, T., Akama, T.K., Guo, L., Craft, M.J., Samy, B., Schavocky, P.J., Watterson, M.D., 2001. Mechanism of glial activation by S100B: involvement of the transcription factor NF κB. Neurobiol. Aging 22, 765–772.

Matsui, T., Mori, T., Tateishi, N., Kagamiishi, Y., Satoh, S., Katsube, N., Morizawa, E., Morimoto, T., Ikuda, F., Asano, T., 2002. Astrocytic activation and delayed infarct expansion after permanent focal ischemia in rats. Part 1: enhanced astrocytic synthesis of S100β in the periinfarct area precedes delayed infarct expansion. J. Cereb. Blood Flow Metab. 22, 711–722.

Murphy, S., 2000. Production of nitric oxide by glial cells: regulation and potential roles in the CNS. Glia 29, 1–13.

Nawashiro, H., Brenner, M., Fukui, S., Shima, K., Hallenbeck, M.J., 2000. High susceptibility to cerebral ischemia in GFAP-null mice. J. Cereb. Blood Flow Metab. 20, 1040–1044.

Pantoni, H.J., Garcia, H.J., 1997. Pathogenesis of leukoaraiosis: a review. Stroke 28, 652–659.

Pettigrew, C.L., Kasner, E.S., Albers, W.G., Gorman, M., Grotta, C.J., Sherman, G.D., Funakoshi, Y., Ishibashi, H., for the arundic acid (ONO-2506) stroke study group, 2006. Safety and tolerability of arundic acid in acute ischemic stroke. J. Neurol. Sci. 251, 50–56.

Roman, C.G., 2005. Vascular dementia prevention: a risk factor analysis. Cerebrovasc. Dis. 20, 91–100.

Sharp, R.F., Lu, A., Tang, Y., Millhorn, E.D., 2000. Multiple molecular penumbras after focal cerebral ischemia. J. Cereb. Blood Flow Metab. 20, 1011–1032.

Shimoda, T., Tateishi, K., Shintaku, K., Yada, N., Katagi, J., Akiyama, T., Maekawa, H., Shinagawa, R., Kondo, K., 1998. ONO-2506, a novel astrocyte modulating agent, suppresses of COX-2 and iNOS mRNA expression in cultured astrocytes and ischemic brain. Abstr.-Soc. Neurosci. 24, 384.

Shinagawa, R., Tateishi, N., Shimoda, T., Maekawa, H., Yada, N., Akiyama, T., Matsuda, S., Katsube, N., 1999. Modulating effects of ONO-2506 on astrocytic activation in cultured astrocytes from rat cerebrum. Abstr.-Soc. Neurosci. 25, 843.

Tateishi, N., Mori, T., Kagamiishi, Y., Satoh, S., Katsube, N., Morizawa, E., Morimoto, T., Matsui, T., Asano, T., 2002. Astrocytic activation and delayed infarct expansion after permanent focal ischemia in rats. part 2: suppression of astrocytic activation by a novel agent (R)-(–)-2-propyloctanoic acid (ONO-2506) leads to mitigation of delayed infarct expansion and early improvement of neurologic deficits. J. Cereb. Blood Flow Metab. 22, 723–734.

Tomimoto, H., Akiguchi, I., Suenaga, T., Nishimura, M., Wakita, H., Nakamura, S., Kimura, J., 1996. Alterations of the blood–brain barrier and glial cells in white matter lesions in cerebrovascular and Alzheimer's disease patients. Stroke 27, 2069–2074.

Tomimoto, H., Ihara, M., Wakita, H., Ohtani, R., Lin, X.J., Akiguchi, I., Kinoshita, M., Shibasaki, H., 2003. Chronic cerebral hypoperfusion induces white matter lesions and loss of oligodendroglia with DNA fragmentation in the rat. Acta Neuropathol. (Berl.) 106, 527–534.

Tsuchiya, M., Sako, K., Yura, S., Yonemasu, Y., 1992. Cerebral blood flow and histopathological changes following permanent bilateral carotid artery ligation in Wistar rats. Exp. Brain Res. 89, 87–92.

Ueno, M., Tomimoto, H., Akiguchi, I., Wakita, H., Sakamoto, H., 2002. Blood–brain barrier is disrupted in the white matter lesions in a rat model of chronic cerebral hypoperfusion. J. Cereb. Blood Flow Metab. 22, 97–104.

Wakita, H., Tomimoto, H., Akiguchi, I., Kimura, J., 1994. Glial activation and white matter changes in the rat brain induced by chronic cerebral hypoperfusion: an immunohistochemical study. Acta Neuropathol. (Berl.) 87, 484–492.

Available online at www.sciencedirect.com
ScienceDirect
Neuroscience Letters xxx (2007) xxx–xxx
Neuroscience Letters
www.elsevier.com/locate/neulet

Capillary beds are decreased in Alzheimer's disease, but not in Binswanger's disease

Hiroshi Kitaguchi [a], Masafumi Ihara [a], Hidemoto Saiki [b], Ryosuke Takahashi [a], Hidekazu Tomimoto [a,*]

[a] *Department of Neurology, Graduate School of Medicine, Kyoto University, Sakyo-ku, Kyoto 606-8507, Japan*
[b] *Department of Neurology, Kitano Hospital, Tazuke Kofukai Medical Research Institute, Osaka 530-8480, Japan*

Received 1 December 2006; received in revised form 23 January 2007; accepted 6 February 2007

Abstract

Morphological abnormalities of the cortical microvessels have been reported in Alzheimer's disease (AD), but not in Binswanger's disease (BD), a form of vascular dementia. Therefore, we compared the capillary beds in AD and BD brains, using a modified Gallyas silver impregnation method and immunohistochemistry for β amyloid. Eight autopsied brains with AD and seven with BD were compared with six control brains. The cortical microvessels in AD were frequently narrowed, and torn off, especially in close proximity to the senile plaques. The capillary densities in AD were significantly decreased as compared with the control brains. In contrast, there were no significant changes in the capillary densities and their morphologies in BD brains. Immunohistochemistry for β amyloid revealed numerous deposits in the vascular wall and perivascular neuropil exclusively in AD brains. Cortical microvascular changes in AD and their absence in BD may indicate a role of β amyloid for the microvessel pathology in AD.

Keywords: Microvessel; Alzheimer's disease; Vascular dementia; Binswanger's disease; Silver impregnation; Amyloid protein

Alzheimer's disease (AD) and vascular dementia are major causes of dementia and disabilities in the elderly. These two conditions have been believed to have an independent pathoetiology. However, in recent studies, co-morbid factors have been revealed in AD and vascular dementia [10,12]. These factors include hypertension, diabetes mellitus, hyperlipidemia, apo E4 ε genotype, cholinergic deficits, and white matter lesions. In addition, patients with vascular lesions reportedly develop dementia more frequently than those without vascular lesions among those subjects with senile changes [18]. Taken together, this evidence has shed light on the interrelationship between AD and vascular dementia, and raised the hypothesis that vascular factors may have a role in the pathogenesis of AD. In concordance with this hypothesis, previous electron microscopic studies have reported thickening of the basement membrane, denervation of the perivascular nerves, and bulging or narrowing of the cortical microvessels in AD brains [14,17].

Binswanger's disease (BD) is a form of vascular dementia, featured by diffuse white matter lesions, lacunar infarcts and fibrohyaline thickening of the microvessel [13]. Fibrohyaline thickening of the microvessels is marked in BD, and significant but less severe in AD in the cerebral white matter [19]. However, with respect to the cortical microvessels, there are no studies in BD. Therefore, we aimed to compare the alterations of the cortical microvessels in AD and BD using a modified Gallyas silver impregnation method and immunohistochemistry for β amyloid, which enable us to examine the network of the brain capillaries, and senile plaques.

We examined 21 brains, including 8 from patients with AD (3 males), 7 from patients with BD (4 males), and 6 from patients who did not have any neuropsychiatric symptoms or brain lesions (3 males). The age was 79 ± 12 years (mean ± S.D.) in the AD, 74 ± 13 years in the BD and 73 ± 4 in the control groups, respectively, among which no significant differences were observed ($p < 0.05$). The brain weight was 1020 ± 111 g in the AD, 1093 ± 112 g in the BD, and 1244 ± 57 g in the control groups, respectively. The brain weight in the AD group was significantly lower than in the control and BD groups ($p < 0.05$). The patients with AD and BD, but not the control patients, met

* Corresponding author. Tel.: +81 75 751 3766; fax: +81 75 751 3766.
E-mail address: tomimoto@kuhp.kyoto-u.ac.jp (H. Tomimoto).

0304-3940/$ – see front matter © 2007 Published by Elsevier Ireland Ltd.
doi:10.1016/j.neulet.2007.02.021